Separation and Purification Technology 237 (2020) 116347

Contents lists available at ScienceDirect

Separation and Purification Technology

journal homepage: www.elsevier.com/locate/seppur

PBI mixed matrix hollow fiber membrane: Influence of ZIF-8 filler over H_2/CO_2 separation performance at high temperature and pressure

Miren Etxeberria-Benavides[a,b,*], Timothy Johnson[c], Shuai Cao[c], Beatriz Zornoza[d,e], Joaquín Coronas[d], Javier Sanchez-Lainez[d], Anahid Sabetghadam[b], Xinlei Liu[b], Eduardo Andres-Garcia[b,g], Freek Kapteijn[b], Jorge Gascon[b,f], Oana David[a,*]

[a] TECNALIA, Parque Tecnológico de San Sebastián, Mikeletegi Pasealekua 2, 20009 Donostia-San Sebastián, Spain
[b] Catalysis Engineering, Chemical Engineering Department, Delft University of Technology, Van der Maasweg 9, 2629 HZ Delft, the Netherlands
[c] Johnson Matthey Technology Centre, Blount's Court, Sonning Common RG4 9NH, United Kingdom
[d] Chemical and Environmental Engineering Department, Instituto de Nanociencia de Aragón (INA) and Instituto de Materiales de Aragón (ICMA), Universidad de Zaragoza-CSIC, 50018 Zaragoza, Spain
[e] Department of Energy and Environment, Instituto de Carboquímica-ICB-CSIC, Miguel Luesma Castán 4, 50018 Zaragoza, Spain
[f] King Abdullah University of Science and Technology, KAUST Catalysis Center, Advanced Catalytic Materials, Saudi Arabia
[g] Instituto de Ciencia Molecular (ICMol), Universitat de València, c/Catedrático José Beltrán, 2, Paterna, 46980, Spain

ARTICLE INFO

Keywords:
H_2/CO_2 separation
Hollow fiber spinning
CO_2 capture
Pre-combustion
Mixed matrix membrane

ABSTRACT

High performance and commercially attractive mixed-matrix membranes were developed for H_2/CO_2 separation via a scalable hollow fiber spinning process. Thin (~300 nm) and defect-free selective layers were successfully created with a uniform distribution of the nanosized (~60 nm) zeolitic-imidazole framework (ZIF-8) filler within the polymer (polybenzimidazole, PBI) matrix. These membranes were able to operate at high temperature (150 °C) and pressure (up to 30 bar) process conditions required in treatment of pre-combustion and syngas process gas streams. Compared with neat PBI hollow fibers, filler incorporation into the polymer matrix leads to a strong increase in H_2 permeance from 65 GPU to 107 GPU at 150 °C and 7 bar, while the ideal H_2/CO_2 selectivity remained constant at 18. For mixed gas permeation, there is competition between H_2 and CO_2 transport inside ZIF-8 structure. Adsorption of CO_2 in the nanocavities of the filler suppresses the transport of the faster permeating H_2 and consequently decreases the H_2 permeance with total feed pressure down to values equal to the pure PBI hollow fibers for the end pressure of 30 bar. Therefore, the improvement of fiber performance for gas separation with filler addition is compromised at high operating feed pressures, which emphasizes the importance of membrane evaluation under relevant process conditions.

1. Introduction

There are several major benefits of membrane based gas separation over conventional gas separation technologies like cryogenic distillation, condensation and amine absorption: (1) lower energy cost since there is no gas-liquid phase change of the gas mixture to be separated, (2) relatively small footprint - gas separation membrane units are smaller than other types of plants, like amine stripping plants, (3) low mechanical complexity and (4) operation under continuous, steady-state conditions [1]. Membrane based gas separation finds additional benefits in pre-combustion application (H_2/CO_2 separation) where stripping and adsorption technologies are limited for direct gas processing [2]. The H_2/CO_2 mixture following typical water-gas shift reactor is at high pressure and high temperature (150–250 °C) conditions. Also, depending on feedstock, the mixture might contain traces of H_2S and steam. Membrane material must be able to operate continuously under such challenging process conditions.

The required hydrogen purity and therefore the membrane material, depends on the specific application, e.g. high purity hydrogen is required for proton exchange membrane fuel cell applications, whereas lower hydrogen purity is required for refinery applications. Due to the unique permeation mechanism, palladium-based membranes show high permeability and exclusive selectivity for H_2 and are commonly used when high purity hydrogen is required [3]. However, their implementation at industrial scale has been hampered due to the low mechanical resistance, modest reproducibility, scale-up problems and

* Corresponding authors.
E-mail addresses: miren.etxeberria@tecnalia.com (M. Etxeberria-Benavides), oana.david@tecnalia.com (O. David).

https://doi.org/10.1016/j.seppur.2019.116347
Received 26 July 2019; Received in revised form 22 November 2019; Accepted 22 November 2019
Available online 23 November 2019

the high fabrication cost of this type of membranes [4,5]. On the other hand, polymeric membranes have been implemented for gas separation on a large scale in industry, mainly due to their easy processing and mechanical strength [6]. Although polymeric membranes are not as selective as inorganic ones, they can be implemented when such a high purity hydrogen is not required. Polymers of intrinsic microporosity (PIMs) have been identified as attractive candidates for gas separation. Their highly rigid and contorted molecular structure leads to inefficient packing of polymer chains and high free volume, and therefore exhibits very high gas permeability [7]. The ultra-high permeability together with interesting CO_2/N_2 and CO_2/CH_4 selectivity, make this PIMs interesting materials for several applications, such as post-combustion CO_2 capture and biogas upgrading. Nonetheless, PIMs present a relatively low selectivity for H_2/CO_2 separation (< 5.5), and in some cases even a reverse selectivity. Few glassy polymers can be successfully used as H_2 selective membranes at the high temperature required in the pre-combustion applications. Polybenzimidazole (PBI) has a rigid polymeric backbone (glass transition temperature of 420 °C) and close chain packing [8], and has already been identified as a good candidate for this application [9–12]. In addition, PBI has shown to exhibit the highest H_2/CO_2 selectivity among the polymer family. Nevertheless, the gas permeation rate through PBI polymer is low [13]. Mixed matrix membranes (MMMs, consisting of a dispersion of filler particles in a polymeric matrix) combine the good processability of polymers with high gas flux and selectivity of the inorganic filler [14,15]. The use of metal-organic frameworks (MOFs) as filler is attractive because of good chemical compatibility with polymers, a high surface area and pore volume, and their porosity is, in general, higher than that of their inorganic counterpart, zeolites. MOFs can be fine-tuned by selecting the appropriate building blocks [16] or by post-synthetic modification [17]. Their partially organic nature improves the polymer/MOF affinity, helping to overcome compatibility issues and avoiding the so-called *sieve-in-a-cage morphology* [18,19]. ZIF-8 is one of the most studied zeolitic imidazolate frameworks, and consists of a metal cation of Zn^{2+} coordinated with the organic linker 2-methylimidazole. ZIF-8 forms a SOD zeolitic topology with large cavities of 11.6 Å size connected through smaller windows of 3.4 Å [20].

Large-scale gas separation applications demand highly productive membranes. Therefore, commercial gas separation membranes are processed into asymmetric structures where a porous support is covered by a very thin dense layer that governs gas permeation. The asymmetric membrane can be a flat film or a hollow fiber. For high productivity, when membranes are packed into modules, a high membrane area/unit volume ratio, i.e. packing density, is desired. Hollow fiber modules offer high packing density (over 10,000 m^2/m^3) [21–23], about ten times higher than for flat sheet (plate and frame) membranes. In addition, hollow fiber membranes can handle very high transmembrane pressure differences (up to 70 bar) and their fabrication costs are 5–20 times lower than those of equivalent membranes for spiral wound modules [24].

This work is focused on the development of commercially relevant membranes (hollow fiber membranes) for CO_2 capture application in pre-combustion processes with a strong focus on performance evaluation under relevant process conditions (30 bar, 150 °C and gas mixtures). Also, considering that the low H_2 permeability is among the major drawbacks of PBI membranes [13], we propose an improved structure with PBI/ZIF-8 based mixed matrix hollow fiber membrane. In this configuration a MOF with high thermal resistance [25,26] would improve the H_2 permeation rate through the PBI matrix. To this date, PBI based hollow fiber membranes reported in the literature have been applied at limited pressures, less than 8 bar. In this way new knowledge on membrane behavior related to real process conditions revealed in this work, are of extreme importance for chemical process industry.

2. Experimental

2.1. Materials

PBI was received from PBI Performance Products INC. as 26 wt% solution in DMAc with 1.5 wt% LiCl. Anhydrous N-methylpyrrolidone (NMP) and dimethylacetamide (DMAc) were purchased from Sigma-Aldrich. Hexane and methanol were purchased from Fisher Scientific. Sylgard 184 (Dow Corning) was used for the defect healing process. Zn $(NO_3)_2$■$6H_2O$, and methanol for ZIF-8 synthesis were purchased from Alfa Aesar. 2-methylimidazole was purchased from Sigma Aldrich. All materials were used without further purification.

2.2. Synthesis of ZIF-8 crystals

ZIF-8 was synthetized as follows. $Zn(NO_3)_2$■$6H_2O$ (98.7 mmol, 29.33 g) and 2-methylimidazole (790.4 mmol, 64.89 g) were dissolved in 2 L methanol at room temperature. The two precursor solutions were then mixed together rapidly and stirred for 30 min. The solution turned turbid gradually. The formed ZIF-8 nanoparticles were collected by centrifugation and washed with fresh methanol three times. The products were dried in ambient air for 16 h. Reaction yield was 8.8 g, 40% based on Zn^{2+}. The samples were activated by subjecting to vacuum at 50 °C for 12 h before N_2 sorption measurement.

2.3. Characterization of ZIF-8 crystals

Powder X-ray diffraction (PXRD) data were collected in reflection geometry using a Bruker AXS D8 diffractometer using Cu Kα radiation (λ = 1.5406 and 1.54439 Å) over the 2θ range 3-130° range in 0.02° steps.

Thermogravimetric analysis (TGA) was conducted between room temperature and 1000 °C heating at 3 °C min^{-1} in an N_2 atmosphere on a Netzsch TG 209 F1 Libra instrument.

Infra-red (IR) spectra were collected on a Perkin Elmer Spectrum One instrument utilizing an UATR attachment. The powder was analyzed directly with no special preparation.

ZIF-8 was subjected to CO_2 and N_2 physisorption analysis. Adsorption/desorption isotherms were collected on a Quantachrome Autosorb iQ instrument. Experiments were conducted at −196 °C (77 K) for N_2 isotherm and 0 °C for CO_2. Both isotherms were subject to BET analysis for surface area calculation. Samples were degassed under vacuum at 125 °C for 16 h.

High-pressure adsorption experiments (up to 35 bar) were performed on a BELSORP-HP. The adsorption/desorption isotherm for CO_2 was obtained with an equilibration time of 1500 s (deviation lower than 0.1% F.S pressure). Temperature ranged from 50 °C to 150 °C. Samples were outgassed overnight under vacuum conditions at 150 °C.

The sample powder was dusted directly onto SEM stubs. The sample was carbon coated prior to analysis to provide a conductive layer for charge dissipation. The sample was analyzed using a Zeiss ultra 55 Field emission electron microscope equipped with in-lens secondary electron and backscatter detectors.

2.4. Preparation of PBI based hollow fiber membranes

The fabrication of PBI based hollow fiber membranes was based on a dry jet followed by wet quench spinning process [23,27–31]. Two types of hollow fibers have been fabricated: (1) hollow fibers based on pure PBI and (2) hollow fibers containing PBI and ZIF-8 filler. This was done by co-extrusion of polymer dope and a bore fluid into a quench bath containing water after a short residence in an air gap. Pure PBI dope was prepared by diluting the 26 wt% starting solution to the desired concentration. Filler containing polymer dope was prepared by dispersing ~10 wt% ZIF-8 into PBI polymer solution under ultrasonic mixing in a bath. ZIF-8 was dried in a vacuum oven at 60 °C for 16 h

Table 1
Spinning parameters for pure PBI and mixed matrix hollow fiber membrane fabrication.

Spinning parameter		Studied range	Pure PBI	PBI-10 wt% ZIF-8
MOF loading	(wt%)	0–10	–	10
PBI concentration	(wt%)	20–22	21.7	20.4
Dope viscosity	cP	–	85,000	76,000*
Bore composition		–	65 DMAc / 35 H_2O	85 NMP/ 15 H_2O
Spinneret temperature	(°C)	20–25	25	20
Outer Dope flow rate	(ml/h)	180–300	240	180
Bore flow rate	(ml/h)	60–80	60	80
Air gap height	(cm)	3.4–20	10	3.4
Quench bath temperature	(°C)	25	25	24
Take up rate	(m/min)	10–30	20	14

Spinneret dimensions: 460 μm inner diameter / 820 μm outer diameter.
* Viscosity for non ZIF-8 loaded dope at same PBI concentration is 55,000 cP.

before use. Dope was loaded into the syringe pump and degassed for 24 h at room temperature before spinning. Polymer dopes were filtered in-line with a 90 μm filter for the pure polymer dopes and 140 μm filter for the filler-containing polymer dopes. At the end, fiber was collected on a drum. Spinning conditions were varied in order to find the optimal combination of spinning parameters for achieving best performance for gas permeation. The studied parameter range and optimal spinning parameters for pure PBI and mixed matrix hollow fiber batches are listed in Table 1. Is important to mention that MOF addition causes an important increase in spinning dope viscosity. The addition of ZIF-8 to the dope containing 20.4 wt% PBI significantly increases dope viscosity, from 55,000 cP for the pure polymer dope to 76,000 cP for 10 wt % ZIF-8 loading. With the objective to have similar viscosity for the two spinning dopes, the optimal PBI concentration was lowered for mixed matrix hollow fiber preparation. Dope viscosity was measured by a Thermo Haake Scientific RS6000 rheometer with 20 mm parallel plate at 25 °C and 10 s^{-1} shear rate. After spinning, fibers were kept in DI water for four days. Water was refreshed every day. Then fibers were washed further in a methanol bath followed by a hexane bath and dried at 70 °C overnight. Hollow fibers were dip-coated for defect healing using a 3 wt% of polydimethylsiloxane (PDMS) in hexane before permeation testing.

2.5. Hollow fiber membrane characterization

The surface and cross-section morphology of the hollow fiber membranes were characterized by scanning electron microscopy (SEM) (Quanta 250 ESEM) equipped with energy dispersive X-ray spectroscopy (EDX). Cross-sections of the membranes were prepared by freeze-fracturing after immersion in liquid nitrogen and subsequently coated with gold/palladium. The low voltage high contrast backscatter electron detector (vCD) and the Everhart Thornley detector (ETD) were used for the analysis of the membranes.

High-pressure adsorption experiments (up to 35 bar) were performed, the same as for ZIF-8 crystals as described in Section 2.3. The adsorption/desorption isotherms for CO_2 were obtained with an equilibration time of 1500 s (deviation lower than 0.1% full scale pressure). Temperature ranged from 50 °C to 150 °C. Samples were outgassed overnight under vacuum conditions at 150 °C.

Hollow fiber gas permeation properties were determined using an experimental set-up based on constant pressure technique [30]. Hollow fiber membrane modules were built by insertion of 1–22 fibers of ~18 cm active length within a tubular stainless-steel container using a method reported in literature [32]. Pure (H_2 and CO_2) and mixed gas permeation experiments (H_2/CO_2 = 50/50 vol%) were carried out in the total feed pressure range of 3.5 to 30 bar at 150 °C. Feed gas flow and pressure was controlled with a Coriolis mass flowmeters (Bronkhorst). Permeate gas flow was measured using a film flow meter (Horiba). To be able to measure the permeate flow of the less permeable component, i.e. CO_2, one module containing 22 pure PBI hollow fibers and one module containing 6 PBI-10 wt% ZIF-8 hollow fibers were tested for pure gases. For mixed gas permeation study, an equimolar H_2/CO_2 gas mixture was fed from the shell side of the fiber and permeate mixture was collected from the lumen side of the fibers in a counter flow configuration. During mixed gas experiments, the stage cut (the ratio between permeate flow rate and feed flow rate) was kept below 1% to avoid concentration polarization phenomena and ensure a constant gas composition at the feed side. This means that maximum permeate flow rate to measure is 100 times lower than the maximum feed flow rate that the permeation system can supply, i.e. maximum 100 mL min^{-1} in our case. Therefore, membrane area was decreased and instead of testing one module with several fibers we tested several modules with one fiber each to have a statistically significant result. An online gas chromatograph (Bruker Scion 456-GC) was used to analyze the permeate stream composition over time. Permeance was calculated once the steady state was reached in the permeate stream of the membrane.

The permeance for gas i was calculated by the following equation:

$$P_i = \frac{F_i}{\Delta f_i \cdot A}$$

where P_i is the gas permeance in gas permeation units (1 GPU = 10^{-6} cm^3 (STP) cm^{-2} s^{-1} $cmHg^{-1}$), F_i is the volumetric flow rate of component i (cm^3 (STP)/s), Δf_i is the partial fugacity difference of component i across the membrane (cmHg) and A is the effective membrane area (cm^2). The use of penetrant fugacity is preferred due to the non-ideal behavior of gases at high pressure [33].

The separation factor or mixed gas selectivity α was calculated as the ratio of the permeance of the more permeable compound i to the permeance of the less permeable compound j:

$$\alpha_{ij} = \frac{P_i}{P_j}$$

3. Results and discussion

3.1. ZIF-8 characterization

Highly porous ZIF-8 materials with good crystal structure were successfully synthesized. Main properties are summarized in Table 2. PXRD, TGA, IR and CO_2 and N_2 physisorption results are found in the supplementary information.

The experimental PXRD pattern for synthesized ZIF-8 nanoparticles (Fig. S1) resembles the simulated pattern, showing that it possesses the right crystal structure. The TG analysis (Fig. S2) shows that the synthesized ZIF-8 nanoparticles are thermally stable up to ~480 °C, above which temperature a gradual decomposition is observed. Infra-red (IR) spectroscopy (Fig. S3) shows the expected bands at ca. 1150 and 1180 cm^{-1} attributed to C-N ring vibrations. The SEM image in Fig. 1 illustrates the individual primary particle sizes of ~60 nm. Ideally, for a highly permeable and gas selective fiber, the outer top layer should be as thin as possible, i.e. ~100 nm. Therefore, ZIF-8 particles with a

Table 2
Review of main properties of ZIF-8 particles.

Parameter	ZIF-8
Crystal structure	Pure phase
Thermal stability	up to ~ 480 °C
Particle size	~60 nm
Surface area	1830 m^2/g

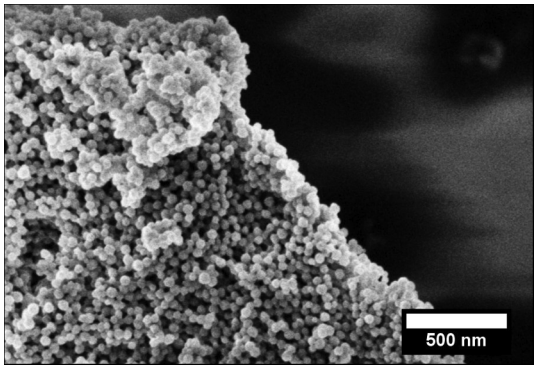

Fig. 1. SEM image of ZIF-8 particles.

particle size below the desired selective layer thickness have been synthesized and used for hollow fiber preparation.

From the N_2 isotherm (Fig. S4) a surface area of 1830 m^2/g was obtained. The CO_2 isotherm presented in the same figure shows that the material has a CO_2 uptake at atmospheric pressure of 1.3 mmol g^{-1}.

3.2. Hollow fibers morphological and structural characterization

SEM images of the outer surface and cross-section of the pure PBI and PBI-10 wt% ZIF-8 mixed matrix hollow fibers are shown in Fig. 2. Both fibers show good circularity and concentricity between the inner and outer diameter (Fig. 2b, e). A porous substructure with small pores and finger-like type macrovoids was obtained (Fig. 2c and f). Both fibers have an outer top layer with a densified structure (Fig. 2a, c). Ideally, for a highly permeable and gas selective fiber, the outer top layer should be as thin as possible, i.e. ~100 nm and completely dense. The substructure of the fiber acts just as support with little resistance to gas transport. For a composite MOF-polymer hollow fiber, the MOF particles should be homogeneously dispersed within the top layer and their size should be smaller than the thickness of the top layer. Therefore, the surface of the mixed matrix hollow fibers was analyzed by the vCD detector at the SEM. The compositional contrast provided by the vCD detector enables observation of the MOF distribution just beneath the surface of the membrane. Small ZIF-8 particles appear with bright contrast in the SEM image of the PBI-10 wt% ZIF-8 hollow fiber outer surface (Fig. 2d). The presence of MOF particles in the outer layer of the fiber was also confirmed by EDX analysis (3.38 wt% Zn).

3.3. Hollow fibers gas permeation

3.3.1. Pure gas permeation -overall analysis

Pure gas transport properties of pure PBI and PBI-10 wt% ZIF-8 mixed matrix hollow fibers are shown in Table 3. A summary of gas permeation results of PBI hollow fiber membranes from literature is included. Pure PBI hollow fibers developed in this work had a permeance of H_2 of 65 GPU and a H_2/CO_2 ideal selectivity of 17.6 at 150 °C and 7 bar transmembrane total fugacity. Asymmetric membranes are defined to be "defect-free" if the ideal selectivity is greater than 80% of the intrinsic selectivity of dense films [34]. If these results are compared with gas permeation through a dense flat film made of pure PBI from the same provider [35] at similar operational conditions (20 Barrer H_2; 20 H_2/CO_2 ideal selectivity), the outer selective top layer has an estimated effective thickness of ~307 nm and the fibers are selective with few or no defects (17.6 versus 20 H_2/CO_2 selectivity). In the calculation of selective layer thickness phenomenon like ageing is not considered, and the resulting value is an estimation. Direct measurement of the selective thickness cannot be performed. Measuring the thickness from SEM pictures only gives a local value (not an average) and in most cases is not easy to identify the borderline between selective layer/transition layer/porous support. A value of ~307 nm for the thickness of the selective top layer is remarkably good. In principle, thinner, up to 100 nm, top layers could be obtained but would require extensive optimization of the spinning recipe. If our results are compared with pure PBI hollow fiber membranes developed by Kumbharkar et al. [10], we obtained an ~100 times higher permeance and 1.4 times higher H_2/CO_2 selectivity. At 250 °C Berchtold et al. [36] achieved 1.7 times higher permeance than us. It is known that temperature has a strong influence over gas permeance through membranes showing an Arrhenius type dependency [12]. The activation energy of H_2 permeability through PBI material is 19.35 kJ mol^{-1} which determines 4 times higher permeance at 250 °C than at 150 °C as previously shown in dense flat sheet PBI membranes [35]. Therefore, if we extrapolate our results at 250 °C we should expect a permeance of 260 GPU.

Upon addition of ZIF-8, the H_2 permeance was increased from 65

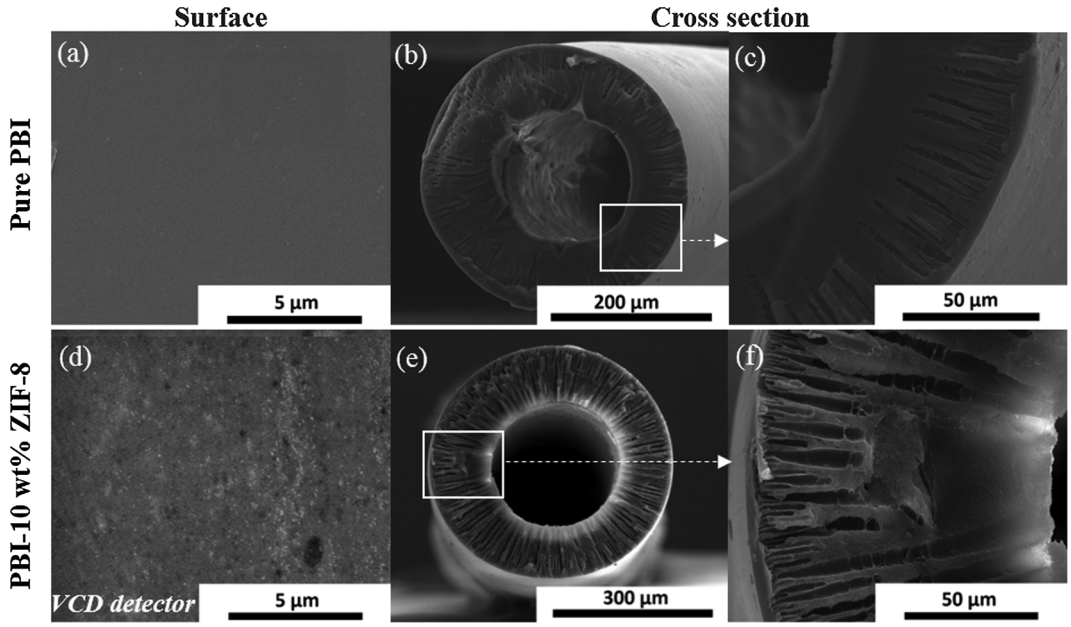

Fig. 2. SEM images of the outer surface and cross-section of the: (a–c) pure PBI hollow fiber, (d–f) PBI-10 wt% ZIF-8 mixed matrix hollow fiber. Surface image of the mixed matrix fiber (d) was obtained by the vCD detector.

Table 3
Transport properties of developed pure PBI and mixed matrix PBI hollow fiber membranes. PBI based hollow fiber membranes reported in literature are also included.

	H_2 permeance (GPU)	H_2/CO_2 selectivity	Testing conditions	Ref.
PBI dense film	20 Barrer	20	150 °C, 3.5 bar, SG	[35]
PBI	65	17.6	150 °C, 7 bar, SG	This work
PBI	0.62	12.8	200 °C, 5–8 bar, SG	[10]
PBI	108	23.7	250 °C, unsp, SG	[36]
PBI-10 wt% ZIF-8	107	16.1	150 °C, 7 bar, SG	This work
PBI-10 wt% ZIF-8/Matrimid	50	11.5	150 °C, 7 bar, MG	[37]
PBI-33 wt% ZIF-8/Matrimid	140	7		
PBI/PdNPs	80	10	60 °C, 1 bar, SG	[38]

SG: single gas test. MG: mixed gas test (50/50 H_2/CO_2). Unsp: unspecified.
1 GPU = 10^{-6} (cm^3(STP))/(cm^2·s·cmHg).

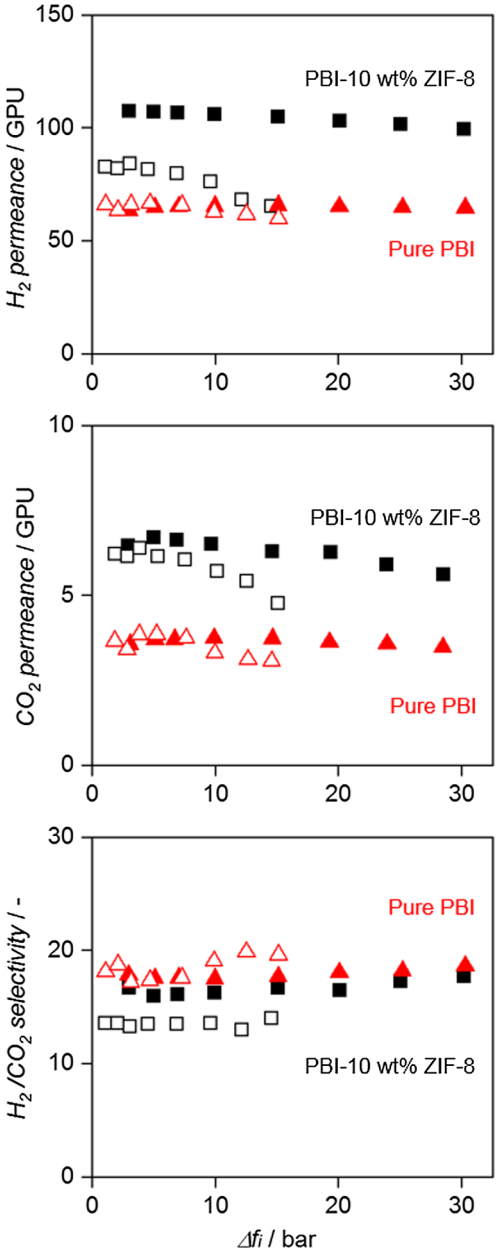

Fig. 3. H_2 and CO_2 permeance and H_2/CO_2 selectivity of pure PBI (*red triangle*) and PBI-10 wt% ZIF-8 (*black square*) hollow fiber membranes as a function of transmembrane partial fugacity of the components. Closed symbols correspond to pure gas experiments and open symbols to mixed gas experiments (H_2/CO_2 = 50/50 vol %). Experiments were performed at 150 °C. (For interpretation of the references to colour in this figure legend, the reader is referred to the web version of this article.)

GPU for the pure PBI to 107 GPU of H_2 for the PBI-10 wt% ZIF-8 fiber, at almost constant H_2/CO_2 ideal selectivity of ~17. This increase in gas permeance could be given by the contribution of following factors: (1) achievement of an even thinner selective top layer when spinning the mixed matrix dope, and/or (2) the contribution from ZIF-8 filler porosity found in the dense top layer and/or (3) a support layer with a more open porous structure. Differences in the pure and mixed gas permeation (see Section 3.3.2) can only be attributed to ZIF-8 contribution. The similar ideal selectivity for H_2/CO_2 separation of PBI-10 wt% ZIF-8 hollow fiber compared with pure PBI hollow fiber shows that the ZIF-8 filler does not act as molecular sieve between the H_2 and CO_2 molecules. The ZIF-8 addition in the selective top layer improves, however, the overall gas permeance. Composite hollow fiber PBI membranes have been previously developed in literature [37,38]. Asymmetric ZIF-8-PBI/Matrimid dual layer hollow fibers were fabricated by Yang et al. [37]. Villalobos et al. [38] proposed a novel scheme to fabricate PBI hollow fiber membranes with a thin skin loaded with fully dispersed palladium nanoparticles. Only modest H_2/CO_2 selectivities are reported compared with the archivable selectivity of PBI material and our results.

3.3.2. Influence of transmembrane fugacity on pure and mixed gas permeations

The influence of transmembrane fugacity (Δf) over gas separation performance of pure PBI and PBI-10 wt% ZIF-8 hollow fiber was evaluated at 150 °C and 3–30 bar using pure and equimolecular CO_2/H_2 mixtures (Fig. 3). H_2 and CO_2 permeances and H_2/CO_2 selectivity are presented as a function of transmembrane fugacity for pure gases (closed symbols) and transmembrane partial fugacity for mixed gas experiments (open symbols). All numeric data are included in Table S1 and S2, supporting information. The H_2 and CO_2 pure gas permeances of pure PBI hollow fibers exhibit little or no dependency on transmembrane fugacity; they stay constant at a level of ~65 GPU and ~3.5 GPU respectively. Therefore, a constant ideal H_2/CO_2 selectivity of ~18 is obtained over the studied fugacity range. Is worth to mention that considering constant CO_2 permeance the typical plasticization phenomena observed for other polyimides like P84® or Matrimid [39,40] did not occur. In the case of PBI-10 wt% ZIF-8 hollow fiber, the H_2 permeance exhibits little or no dependency on transmembrane fugacity, while a slight decrease in CO_2 permeance is observed as fugacity increases. As a result, a slight increase in the ideal H_2/CO_2 selectivity is observed as transmembrane fugacity increases (from 16.6 at 3 bar to 17.7 at 30 bar).

For mixed gas permeation, the same separation performance is obtained for pure PBI hollow fibers. It shows that neither H_2 permeance nor CO_2 permeance is affected by the presence of the other gas. However, a significant deviation of mixed gas permeation from pure gas permeation is observed when adding 10 wt% ZIF-8. The H_2 mixed gas permeance is much lower than the H_2 pure gas permeance (23% lower at 3 bar total fugacity). At the same time, the H_2 permeance remains

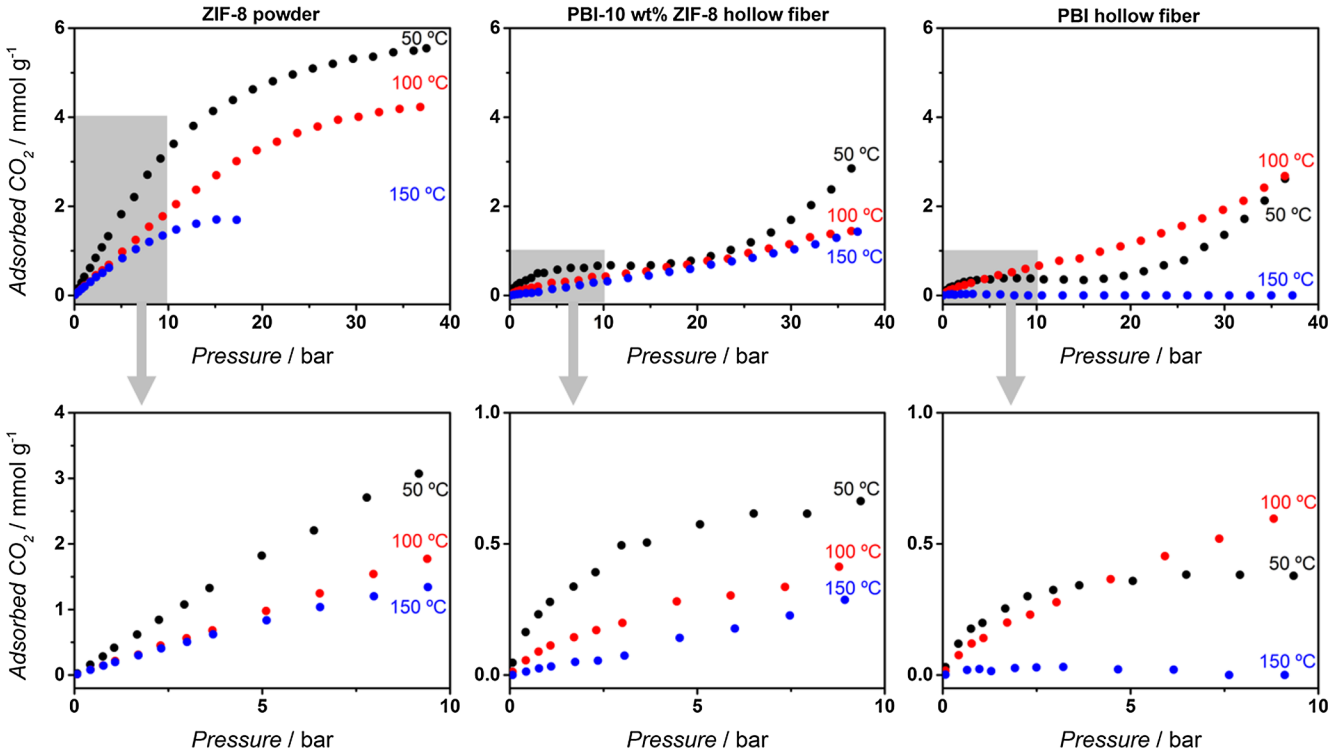

Fig. 4. High pressure adsorption isotherms (excess adsorption) for carbon dioxide on ZIF-8 powder (*left*), PBI-10 wt% ZIF-8 hollow fiber (*middle*) and pure PBI hollow fiber (*right*), at 50 °C (*black*), 100 °C (*red*) and 150 °C (*blue*). (For interpretation of the references to colour in this figure legend, the reader is referred to the web version of this article.)

constant at a value of ~83 GPU up to 5 bar partial fugacity, above which it starts to decrease to the level of pure PBI hollow fibers at 15 bar (~65 GPU). There is a smaller effect of fugacity on the CO_2 mixed gas permeance which starts from the same value as for pure gas permeance and decreases from 6.2 to 4.8 GPU as the fugacity increases. This phenomenon is attributed to the competitive sorption between H_2 and CO_2 gas molecules. CO_2 molecules are adsorbed in the cavities of ZIF-8 particles and therefore transportation of H_2 molecules through ZIF-8 diffusion pathways is reduced [37,41]. Adsorption and diffusion of gases in ZIF-8 by molecular simulation studies have been reported in literature, where enhanced adsorption in specific sites was determined [42]. Two preferred adsorption sites were identified for H_2. The first adsorption site is located on top of the imidazolate ring over the C=C bond and the second adsorption site at the center of the hexagonal window. For CO_2, the preferred adsorption site may depend on CO_2 loading [43]. At low loading, CO_2 is adsorbed in the vicinity of the C=C bond of the 2-methylimidazolate linker. At high loading CO_2 is also adsorbed near the aperture and in the central cage. It means that as the pressure increases, the nanocages of ZIF-8 are saturated (mainly by CO_2) and therefore both pathways for CO_2 and H_2 diffusion through ZIF-8 may be hindered. The stronger adsorption of CO_2 (see Section 3.4) suppresses the H_2 permeation in the mixture, yielding a lower mixture selectivity, but compensates partly for the hindered diffusivity, explaining the smaller permeance reduction. This result shows, unlike other MOF fillers, the active role of ZIF-8 in the MMM and also demonstrates that a possible void space between filler and polymer does not play a role in this system [44], otherwise a selectivity equal to the pure PBI would have been observed. Summarizing, at lower pressures transport through the ZIF-8 contributes to the permeation, while at higher pressures this contribution is reduced by strong adsorption of penetrants.

Is worth mentioning that this performance is reversible. When the fugacity was decreased to the initial testing value of 3 bar, the initial permeance values were recovered (see Table S1).

3.4. Hollow fibers gas sorption measurements

Fig. 4 shows the results from the adsorption measurements of the three samples (ZIF-8 powder, pure PBI hollow fiber and PBI-10 wt% ZIF-8 hollow fiber) at different temperatures (50, 100 and 150 °C) in a pressure range of 0 to 35 bar.

ZIF-8 powder (Fig. 4 *left*) exhibits an isotherm that is concave to the pressure axis, with a larger slope in the low-pressure range (0–20 bar). The adsorption capacity decreases with increasing temperature, in agreement with the exothermal adsorption process. As expected, ZIF-8 presents a much higher adsorption than pure PBI, attributed to the high specific surface area of MOF particles.

Interpretation of pure PBI polymer behavior becomes more complex. Sorption isotherms in glassy polymers can be described as *type II* according to IUPAC [45] with an S-shape character, *i.e.* concave to the pressure axis at the beginning, then almost linear and finally convex to the pressure axis. The complete isotherm can be reached at low temperatures and/or high pressures [46]. In our case only at 50 °C the isotherm is completed (Fig. 4 *right*). The adsorbed CO_2 amount decreases with increasing temperature at pressures below 5 bar. However, at higher pressures the profile at 50 °C lies below the one at 100 °C. This behavior cannot be explained in terms of thermodynamics, and so kinetic effects, i.e. diffusion limitations, must be considered. Mobility of CO_2 and polymer chains is improved at higher temperature. This effect was already reported in literature for polyethyleneimine [47]. The nearly absent CO_2 adsorption at 150 °C is expected based on thermodynamics.

PBI-10 wt% ZIF-8 hollow fiber experimental isotherms are shown in Fig. 4 *middle*. The adsorption profiles have contributions from both components, but an exact match is not expected due to unknown interaction between the constituents: *i.e.* the interface between polymer and MOF particles, differences in the surface roughness and porosity between the neat PBI and mixed matrix fiber. H_2 adsorption could not be determined within the equipment's accuracy. These results support

the picture of the mixed matrix membrane behavior, where the adsorption of CO_2 in the ZIF-8 still plays a role at 150 °C and high pressure. Therefore it is expected that operation at higher temperatures further reduce this adsorption, leading to higher H_2/CO_2 selectivities (next to higher permeances), as is observed in literature for pure PBI.

4. Conclusions

Defect-free hollow PBI fibers with thin (~300 nm) top dense mixed matrix layers containing a uniform distribution of the nanosized (~60 nm) zeolitic-imidazole framework filler (ZIF-8) in the polymer polybenzimidazole (PBI) matrix. The protocol developed could be used for the incorporation of any type of porous filler. ZIF-8 incorporation into the PBI polymer matrix strongly influences gas transport, specifically in mixed gas permeation, where the improvement of fiber performance for H_2/CO_2 separation with filler addition is compromised at high operating feed pressures (30 bar) and 150 °C due to competitive adsorption of CO_2 in ZIF-8, blocking the transport. The ZIF-8 plays an active role in the permeation performance, unlike many other fillers. We expect that at higher temperature the H_2/CO_2 selectivity will improve due to lower CO_2 adsorption in the filler. Our results reveal material performance under conditions relevant to the application and demonstrate the importance of such an evaluation. Future improvement of membrane performance is foreseen by incorporation of porous fillers with lower interaction with CO_2 and higher size exclusion properties for H_2/CO_2, like Benzimidazole-linked polymers (BILPs), a new class of porous organic framework [48].

CRediT authorship contribution statement

Miren Etxeberria-Benavides: Conceptualization, Investigation, Methodology, Writing - original draft, Writing - review & editing. **Timothy Johnson:** Methodology, Writing - review & editing. **Shuai Cao:** Investigation, Methodology, Writing - review & editing. **Beatriz Zornoza:** Investigation, Writing - review & editing. **Joaquín Coronas:** Writing - review & editing, Funding acquisition. **Javier Sanchez-Lainez:** Investigation, Writing - review & editing. **Anahid Sabetghadam:** Investigation, Writing - review & editing. **Xinlei Liu:** Investigation, Writing - review & editing. **Eduardo Andres-Garcia:** Investigation, Writing - review & editing. **Freek Kapteijn:** Writing - review & editing, Supervision, Funding acquisition. **Jorge Gascon:** Writing - review & editing, Supervision, Funding acquisition. **Oana David:** Conceptualization, Methodology, Writing - review & editing, Supervision.

Declaration of Competing Interest

The authors declare that they have no known competing financial interests or personal relationships that could have appeared to influence the work reported in this paper.

Acknowledgements

The authors acknowledge the financial support of the European Research Council under the European Union's Seventh Framework Programme (FP/2007-2013), under grant agreement no. 608490, M^4CO_2 project. The Laboratorio de Microscopías Avanzadas (LMA) at INA, University of Zaragoza is also acknowledged.

Appendix A. Supplementary material

Supplementary data to this article can be found online at https://doi.org/10.1016/j.seppur.2019.116347.

References

[1] P. Bernardo, E. Drioli, G. Golemme, Membrane gas separation: a review/state of the art, Ind. Eng. Chem. Res. 48 (2009) 4638–4663, https://doi.org/10.1021/ie8019032.
[2] O.C. David, D. Gorri, A. Urtiaga, I. Ortiz, Mixed gas separation study for the hydrogen recovery from H2/CO/N2/CO2 post combustion mixtures using a Matrimid membrane, J. Memb. Sci. 378 (2011) 359–368, https://doi.org/10.1016/j.memsci.2011.05.029.
[3] E. Fernandez, K. Coenen, A. Helmi, J. Melendez, J. Zuñiga, D.A. Pacheco Tanaka, M. van Sint Annaland, F. Gallucci, Preparation and characterization of thin-film Pd–Ag supported membranes for high-temperature applications, Int. J. Hydrogen Energy 40 (2015) 13463–13478, https://doi.org/10.1016/j.ijhydene.2015.08.050.
[4] J. Gascon, F. Kapteijn, B. Zornoza, V. Sebastián, C. Casado, J. Coronas, Practical approach to zeolitic membranes and coatings: state of the art, opportunities, barriers, and future perspectives, Chem. Mater. 24 (2012) 2829–2844, https://doi.org/10.1021/cm301435j.
[5] J. Coronas, Present and future synthesis challenges for zeolites, Chem. Eng. J. 156 (2010) 236–242, https://doi.org/10.1016/j.cej.2009.11.006.
[6] M.A. Aroon, A.F. Ismail, T. Matsuura, M.M. Montazer-Rahmati, Performance studies of mixed matrix membranes for gas separation: a review, Sep. Purif. Technol. 75 (2010) 229–242, https://doi.org/10.1016/j.seppur.2010.08.023.
[7] Neil B. McKeown, Polymers of intrinsic microporosity, ISRN Mater. Sci. 2012 (2012) 16, https://doi.org/10.5402/2012/513986.
[8] S.C. Kumbharkar, P.B. Karadkar, U.K. Kharul, Enhancement of gas permeation properties of polybenzimidazoles by systematic structure architecture, J. Memb. Sci. 286 (2006) 161–169, https://doi.org/10.1016/j.memsci.2006.09.030.
[9] R.P. Singh, G.J. Dahe, K.W. Dudeck, C.F. Welch, K.A. Berchtold, High temperature polybenzimidazole hollow fiber membranes for hydrogen separation and carbon dioxide capture from synthesis gas, Energy Procedia 63 (2014) 153–159, https://doi.org/10.1016/j.egypro.2014.11.015.
[10] S.C. Kumbharkar, Y. Liu, K. Li, High performance polybenzimidazole based asymmetric hollow fibre membranes for H2/CO2 separation, J. Memb. Sci. 375 (2011) 231–240, https://doi.org/10.1016/j.memsci.2011.03.049.
[11] D.R. Pesiri, B. Jorgensen, R.C. Dye, Thermal optimization of polybenzimidazole meniscus membranes for the separation of hydrogen, methane, and carbon dioxide, J. Memb. Sci. 218 (2003) 11–18, https://doi.org/10.1016/S0376-7388(03)00129-7.
[12] J. Sánchez-Laínez, B. Zornoza, C. Téllez, J. Coronas, Asymmetric polybenzimidazole membranes with thin selective skin layer containing ZIF-8 for H2/CO2 separation at pre-combustion capture conditions, J. Memb. Sci. 563 (2018) 427–434, https://doi.org/10.1016/j.memsci.2018.06.009.
[13] T.-S. Chung, A critical review of polybenzimidazoles, J. Macromol. Sci. Part C. 37 (1997) 277–301, https://doi.org/10.1080/15321799708018367.
[14] P.S. Goh, A.F. Ismail, S.M. Sanip, B.C. Ng, M. Aziz, Recent advances of inorganic fillers in mixed matrix membrane for gas separation, Sep. Purif. Technol. 81 (2011) 243–264, https://doi.org/10.1016/j.seppur.2011.07.042.
[15] B. Seoane, J. Coronas, I. Gascon, M.E. Benavides, O. Karvan, J. Caro, F. Kapteijn, J. Gascon, Metal–organic framework based mixed matrix membranes: a solution for highly efficient CO2 capture? Chem. Soc. Rev. 44 (2015) 2421–2454, https://doi.org/10.1039/C4CS00437J.
[16] J. Gascon, U. Aktay, M. Hernandezalonso, G. Vanklink, F. Kapteijn, Amino-based metal-organic frameworks as stable, highly active basic catalysts, J. Catal. 261 (2009) 75–87, https://doi.org/10.1016/j.jcat.2008.11.010.
[17] Z. Wang, S.M. Cohen, Postsynthetic modification of metal-organic frameworks, Chem. Soc. Rev. 38 (2009) 1315–1329, https://doi.org/10.1039/B802258P.
[18] R. Mahajan, R. Burns, M. Schaeffer, W.J. Koros, Challenges in forming successful mixed matrix membranes with rigid polymeric materials, J. Appl. Polym. Sci. 86 (2002) 881–890, https://doi.org/10.1002/app.10998.
[19] Rajiv Mahajan, De Q. Vu, William J. Koros, Mixed matrix membrane materials: an answer to the challenges faced by membrane based gas separations today? J. Chinese Inst. Chem. Eng. 33 (2002) 77–86.
[20] K.S. Park, Z. Ni, A.P. Côté, J.Y. Choi, R. Huang, F.J. Uribe-Romo, H.K. Chae, M. O'Keeffe, O.M. Yaghi, Exceptional chemical and thermal stability of zeolitic imidazolate frameworks, Proc. Natl. Acad. Sci. 103 (2006), https://doi.org/10.1073/pnas.0602439103 10186 LP – 10191.
[21] M.F.A. Wahab, A.F. Ismail, S.J. Shilton, Studies on gas permeation performance of asymmetric polysulfone hollow fiber mixed matrix membranes using nanosized fumed silica as fillers, Sep. Purif. Technol. 86 (2012) 41–48, https://doi.org/10.1016/j.seppur.2011.10.018.
[22] S. Husain, W.J. Koros, Mixed matrix hollow fiber membranes made with modified HSSZ-13 zeolite in polyetherimide polymer matrix for gas separation, J. Memb. Sci. 288 (2007) 195–207, https://doi.org/10.1016/j.memsci.2006.11.016.
[23] N. Peng, N. Widjojo, P. Sukitpaneenit, M.M. Teoh, G.G. Lipscomb, T.-S. Chung, J.-Y. Lai, Evolution of polymeric hollow fibers as sustainable technologies: past, present, and future, Prog. Polym. Sci. 37 (2012) 1401–1424, https://doi.org/10.1016/j.progpolymsci.2012.01.001.
[24] Richard W. Baker, Membrane Technology and Applications, 2nd ed. Membr. Technol. Appl., 2004. http://adsabs.harvard.edu/abs/2004mta..book.....B.
[25] P.K. Thallapally, N. Martin, S.K. Nune, P.K. Thallapally, A. Dohnalkova, C. Wang, Synthesis and properties of nano zeolitic imidazolate frameworks, Chem. Commun. 46 (2010) 4878–4880, https://doi.org/10.1039/c002088e.
[26] J.B. James, Y.S. Lin, Thermal stability of ZIF-8 membranes for gas separations, J. Memb. Sci. 532 (2017) 9–19, https://doi.org/10.1016/j.memsci.2017.02.017.
[27] Y. Li, T. Chung, Z. Huang, S. Kulprathipanja, Dual-layer polyethersulfone (PES)/

BTDA-TDI/MDI co-polyimide (P84) hollow fiber membranes with a submicron PES–zeolite beta mixed matrix dense-selective layer for gas separation, J. Memb. Sci. 277 (2006) 28–37, https://doi.org/10.1016/j.memsci.2005.10.008.
[28] N. Widjojo, T.-S. Chung, S. Kulprathipanja, The fabrication of hollow fiber membranes with double-layer mixed-matrix materials for gas separation, J. Memb. Sci. 325 (2008) 326–335, https://doi.org/10.1016/j.memsci.2008.07.046.
[29] O. David, Y. Gendel, M. Wessling, Tubular macro-porous titanium membranes, J. Memb. Sci. 461 (2014) 139–145, https://doi.org/10.1016/j.memsci.2014.03.010.
[30] O.C. David, D. Gorri, K. Nijmeijer, I. Ortiz, A. Urtiaga, Hydrogen separation from multicomponent gas mixtures containing CO, N2 and CO2 using Matrimid® asymmetric hollow fiber membranes, J. Memb. Sci. 419–420 (2012) 49–56, https://doi.org/10.1016/j.memsci.2012.06.038.
[31] V.P. Babu, B.E. Kraftschik, W.J. Koros, Crosslinkable TEGMC asymmetric hollow fiber membranes for aggressive sour gas separations, J. Memb. Sci. 558 (2018) 94–105, https://doi.org/10.1016/j.memsci.2018.04.028.
[32] D.Q. Vu, W.J. Koros, S.J. Miller, High pressure CO2/CH4 separation using carbon molecular sieve hollow fiber membranes, Ind. Eng. Chem. Res. 41 (2002) 367–380, https://doi.org/10.1021/ie010119w.
[33] B. Freeman, Y. Yampolskii, I. Pinnau, Materials Science of Membranes for Gas and Vapor Separation, 2006.
[34] S.C. Pesek, W.J. Koros, Aqueous quenched asymmetric polysulfone membranes prepared by dry/wet phase separation, J. Memb. Sci. 81 (1993) 71–88, https://doi.org/10.1016/0376-7388(93)85032-R.
[35] X. Li, R.P. Singh, K.W. Dudeck, K.A. Berchtold, B.C. Benicewicz, Influence of polybenzimidazole main chain structure on H2/CO2 separation at elevated temperatures, J. Memb. Sci. 461 (2014) 59–68, https://doi.org/10.1016/j.memsci.2014.03.008.
[36] K.A. Berchtold, K.W. Dudeck, R.P. Singh, G.J. Dahe, Polybenzimidazole hollow fiber membranes and method for making an asymmetric hollow fiber membrane, US2016375410 (A1), 2016.
[37] T. Yang, G.M. Shi, T.-S. Chung, Symmetric and asymmetric zeolitic imidazolate frameworks (ZIFs)/polybenzimidazole (PBI) nanocomposite membranes for hydrogen purification at high temperatures, Adv. Energy Mater. 2 (2012) 1358–1367, https://doi.org/10.1002/aenm.201200200.
[38] L.F. Villalobos, R. Hilke, F.H. Akhtar, K.-V. Peinemann, Fabrication of polybenzimidazole/palladium nanoparticles hollow fiber membranes for hydrogen purification, Adv. Energy Mater. 8 (2018) 1701567, https://doi.org/10.1002/aenm.201701567.
[39] A. Bos, I.G.M. Pünt, M. Wessling, H. Strathmann, CO2-induced plasticization phenomena in glassy polymers, J. Memb. Sci. 155 (1999) 67–78, https://doi.org/10.1016/S0376-7388(98)00299-3.
[40] J.N. Barsema, G.C. Kapantaidakis, N.F.A. van der Vegt, G.H. Koops, M. Wessling, Preparation and characterization of highly selective dense and hollow fiber asymmetric membranes based on BTDA-TDI/MDI co-polyimide, J. Memb. Sci. 216 (2003) 195–205, https://doi.org/10.1016/S0376-7388(03)00071-1.
[41] J.-R. Li, Y. Ma, M.C. McCarthy, J. Sculley, J. Yu, H.-K. Jeong, P.B. Balbuena, H.-C. Zhou, Carbon dioxide capture-related gas adsorption and separation in metal-organic frameworks, Coord. Chem. Rev. 255 (2011) 1791–1823, https://doi.org/10.1016/j.ccr.2011.02.012.
[42] B. Assfour, S. Leoni, G. Seifert, Hydrogen adsorption sites in zeolite imidazolate frameworks ZIF-8 and ZIF-11, J. Phys. Chem. C. 114 (2010) 13381–13384.
[43] L. Zhang, G. Wu, J. Jiang, Adsorption and diffusion of CO2 and CH4 in zeolitic imidazolate framework-8: effect of structural flexibility, J. Phys. Chem. C. 118 (2014) 8788–8794, https://doi.org/10.1021/jp500796e.
[44] R. Semino, J.C. Moreton, N.A. Ramsahye, S.M. Cohen, G. Maurin, Understanding the origins of metal–organic framework/polymer compatibility, Chem. Sci. 9 (2018) 315–324, https://doi.org/10.1039/C7SC04152G.
[45] K.S.W. Sing, D.H. Everett, R.A.W. Haul, L. Moscou, R.A. Pierotti, J. Rouquerol, T. Siemieniewska, Reporting physisorption data for gas/solid systems, Handb. Heterog. Catal. (2008), https://doi.org/10.1002/9783527610044.hetcat0065.
[46] M. Lanč, K. Pilnáček, C.R. Mason, P.M. Budd, Y. Rogan, R. Malpass-Evans, M. Carta, B.C. Gándara, N.B. McKeown, J.C. Jansen, O. Vopička, K. Friess, Gas sorption in polymers of intrinsic microporosity: the difference between solubility coefficients determined via time-lag and direct sorption experiments, J. Memb. Sci. 570–571 (2019) 522–536, https://doi.org/10.1016/j.memsci.2018.10.048.
[47] R. Sanz, G. Calleja, A. Arencibia, E.S. Sanz-Pérez, CO2 adsorption on branched polyethyleneimine-impregnated mesoporous silica SBA-15, Appl. Surf. Sci. 256 (2010) 5323–5328, https://doi.org/10.1016/j.apsusc.2009.12.070.
[48] M. Shan, X. Liu, X. Wang, I. Yarulina, B. Seoane, F. Kapteijn, J. Gascon, Facile manufacture of porous organic framework membranes for precombustion CO_2 capture, Sci. Adv. 4 (2018), http://advances.sciencemag.org/content/4/9/eaau1698.abstract.